

BOX GIRDER OVERPASS PRE-TEST FINAL ELEMENT MODELING APPLICATION FOR BRIDGE CONDITION ASSESSMENT

^{1*} Kumar Priyadarsini, ²Nihar Jha

^{1*} Professor, Dept. OF Civil Engineering, NIT BBSR,

Asst. Professor Dept. of Civil Engineering, BCE, BBSR

^{1*} priyadarsinikumkum@gmail.com, nihar99@gmail.com

ABSTRACT: Due to financial limitations and traffic disruptions, it is not always possible to load test bridges with known truck loads for assessment purposes. This work illustrates the goals and advantages of an initial finite element model (FEM) of a reinforced concrete box girder in order to address these concerns. An in-depth FEM of the bridge's "as-new" condition is first given, and parameters to include in the FEM before and after model update are then identified. The scheme's preparation for field testing utilising pre-test FEM data is then demonstrated. The bridge's first two mode shapes, lateral and longitudinal sway, were present, whereas the third and fourth modes, flexural and torsional, respectively, were. Prior to model update, it was discovered that the regulating parameters—variation in girder cross section, supports fixity at abutment, and pier—had a considerable impact on the modal features. Decisions about the excitation source, instrumentation strategy, and modal analysis methods for field testing that will take place soon were determined based on the modal model of the bridge.

KEYWORDS: Box Girder, Finite Element Model, Ambient Vibration, Field Test, Modal Analysis

1 INTRODUCTION

Bridges are regarded as communication arteries and make up a sizable section of infrastructure. Longer and heavier vehicles are used as a result of industrial expansion, which increases the loading on deteriorating bridges. In Australia, bridge construction is crucial for economic growth. Furthermore, interstate freight traffic has been growing steadily since 2000 and is predicted to reach 280 billion tones per km by 2020 [1]. In order to accommodate heavier loadings on Australian road networks, the SM1600 (160t) design truck, debuted in 2004, is currently employed. More than 80% of bridge networks, however, are created using older Design Classes, like T44 (44t) and H20-S16 [2]. AASHTO LRFD [3] and AS5100.5 [4] are two bridge design specifications that go into great detail about how to analyse a bridge's strength and serviceability using computer modelling. In post-design evaluation, bridge inspection guidelines such as Transport and Main Road (TMR) assessment methodology, the need for Finite Element Model (FEM) is highlighted for less conservative and more accurate results [5].

In the field of Structural Health Monitoring (SHM), bridge structural assessment is basically conducted by externally exciting the bridge and recording the response due to the excitation with the help of sensory apparatus. Using available analysing techniques, modal parameters such as natural frequencies and mode shapes are extracted from recordings. Model updating is a process that minimizes the different between analytical and experimental measurements. Concept of model updating is illustrated in Figure 1. The level of accuracy in updated FEM mainly rests upon the initial FEM and field measurements.

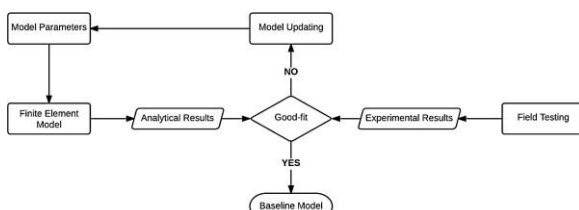


Figure 1: Process of FEM model updating

Very limited number of updating parameters need to be selected to avoid an ill-conditioned model [6]. Factors related to inaccuracy in the FEM are mainly physical errors such as material properties, geometrical errors such as boundary conditions and modelling errors such as discretization errors [6-8]. To validate the reliability of updated FEM, systematic comparison is made between experimental and analytical model. Natural Frequency Difference (NFD) and Modal Assurance Criteria (MAC) are examples of methods used for modal parameters comparison [9].

Despite the numerous reports in the literature on FEM studies associated with field tests, very limited studies

have investigated a systematic way of using an initial FEM for model updating and field test planning of Reinforced Concrete (RC) box girder bridge. This paper aims to show that pre-test FEM can effectively evaluate FEM updating parameters and suitably simulate field test preparation. To address this objective, FEM is analysed to obtain dynamic and static bridge responses. Modelling parameters which affect the fundamental frequencies and mode shapes of bridge are identified for future model updating. Eventually, suitable sensing system, excitation source and modal analysis techniques are proposed for actual field test.

2 DEVELOPMENT OF FEM

Bridge of interest is a multi-cellular reinforced concrete (RC) box girder bridge located in Linkfield road, Brisbane, Queensland. It is composed of two spans each having a span length of 25.3m with an integral wall-type pier in the middle and it was originally designed for AASHO H20-S16 vehicle loading at 1971 [10]. The bridge was modelled using grillage-analogy method under private contract for TMR to assess the performance of bridge with different design vehicles. Modal results of grillage analysis are used as reference for FEM, because currently no field measurements are available for validation.

The first six natural frequencies and mode shapes using free vibration Eigenvector analysis are shown in Table 1.

Table 1: Mode shapes and fundamental frequencies of initial FEM (obtained in CSiBridge®)

Mode shape	Frequency (Hz)
1 st mode-Sway lateral direction	0.769
2 nd mode-Sway longitudinal direction	0.808
3 rd mode-First bending	3.802
4 th mode-First torsion	4.513
5 th mode-Second bending	5.336
6 th mode-Second torsion	8.870

Influence of different parameters on global behaviour of bridge, viz. fundamental frequencies and mode shapes are investigated to find out which parameters have significant effect. Since first flexural and torsional modes occur within the first four modes, modes 1 to 4 were chosen as thresholds (limiting ranges) for comparison.

NON-STRUCTURAL EFFECT

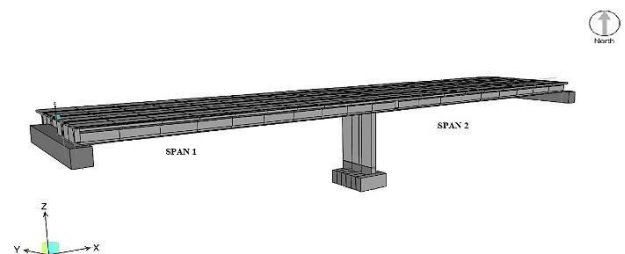
Grade of road at start of span one is -1.3% and it reduces to -0.8% at end of span two. When road slope is considered in the FEM, very marginal changes in the frequency occurred. Only the frequency of the 4th mode which is a torsion mode experienced some reduction. This is due to the fact that road slope creates some elevation in the deck, and hence the stress distribution changes. Road slope is more prevalent in curved bridges for analysis of centrifugal forces. Nonetheless, road slope affects the load rating and must be included in bridge assessment [11].

Abutments have skew angle of 5.81°, while central pier is straight to align with road underneath. Skew angle was taken into account in FEM and a minor effect was observed. Order of mode shapes changed because of skewed support, whereby first mode became longitudinal sway and second mode changed to lateral sway lateral. Generally when skew angle at supports is more than 45°, appropriate provisions in terms of direction of meshing and element connectivity should be provided to consider torsional effect due to skewness and to correctly define the load paths [12]. Abutment skewness can therefore be ignored at this stage of modelling.

Original mesh size for initial FEM was set to 1.2m. Finer mesh size, viz. 1m, 0.25m and 0.1 m were implemented to investigate how the accuracy of model improves. First mode was hugely affected by mesh size and a reduction in frequency up to 24% occurred when the maximum mesh size was set to 0.1m. It should be mentioned that computation time substantially increases for finer mesh size. Higher mesh quality is used for design of bridges with complex geometry and highly-skewed supports. In the case of dynamic analysis, coarser mesh size is reasonable, because degree of mesh refinement should be sufficient to maintain proper mass distribution [11]. Therefore, mesh size between 0.75m to 1.2m was considered sufficient for preliminary FEM analysis.

It is stated in the design drawings that cantilever footway was cast after removal of supports for deck and then kerbs and parapets were cast. On both sides of the deck there are cast in-situ cantilever footways. To find out the contribution of these non-structural members on modal parameters, cantilever portion of bridge was entirely removed. Interestingly, it was found that exclusion of cantilever footway had marginal effect on frequencies and mode shapes, indicating that cantilever portion has no contribution to deck stiffness. In the second scenario, the kerbs and parapets at both sides were included in FEM. Less than 2% change in the frequencies of the first four modes was observed due to addition of superimposed dead loads. Reduction in frequencies except flexural mode was noticeable due to the addition of deck wearing on superstructure. It can be stated that cantilever footway can be removed from initial FEM. Effect of kerb, parapet and wearing surface can be considered as superimposed dead load in updated model.

VARIATIONS IN DECK CROSS SECTION



Typical cross section of cellular deck and full 3D FEM are illustrated in Figure 2. Deck has inclination of -2% towards the cantilever footway. Due to gradient change, height of deck at southern side is 1.143m and 0.987 at northern side. First flexural and torsional modes are more affected by change in deck height. This could be due the stability of girders when subjected to out-of- plane movement in third and fourth vibrational modes. As stated earlier for

road slope, gradient of superstructure can be ignored in dynamic analysis. Hence, average deck height without considering cross-fall is reasonable for initial FEM.

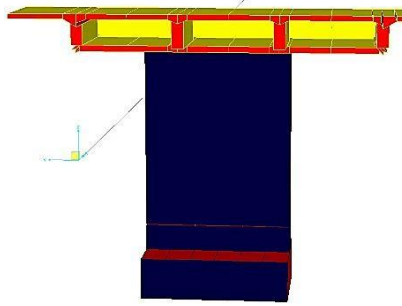


Figure 2. 3D rendered view and cross section of box girder at central pier

Alteration in interior and exterior web thickness affects girder spacing. Web thickness is 0.381m at both abutments and reduces to 0.203m over 6.9m and then increases to 0.457m at pier diaphragms over 10.4m. Webs with nominal thickness of 0.347 was assumed for initial FEM. Minimal changes in frequency noticed for web thickness of 0.203m to 0.457m. When web thickness is set to 0.457m as average value, the first mode was in longitudinal direction since the abutments became stiffer and hence resisted the lateral movement. The main reason is that mass of superstructure increases when the variation of web thickness is taken into account. As the result, the frequency decreases since it is inversely proportional to change in mass. Thus, alteration in web thickness should be incorporated in updated model to accurately capture the dynamic response.

Top slab thickness is constant at 0.152m. For bottom slab, thickness is 0.140m at abutments and through midspan and increases to 0.203m towards central pier. Similarly, bottom slab has more influence on model when complete variations are modelled in FEM. When entire variation in bottom slab thickness was adopted for FEM, modal data changed up to 5%. This emphasises the importance of including the cross-section variations which must be considered in initial FEM.

EFFECT OF BOUNDARY CONDITIONS

Due to unavailability of manufacture's specifications, the fixity of supports at abutment and pier were adopted

based on grillage model. The first three letters are translation along global Z, Y, X axes, while the second three letters are rotation about global Z, Y, X axes. In initial FEM, fixity of bearing at abutments is taken to be FRRFFR, while bearing at pier was FFFRRR. In addition, fully fixed support (FFFFFF) conditions are used in lieu of piles that were well-driven into hard soil stratum.

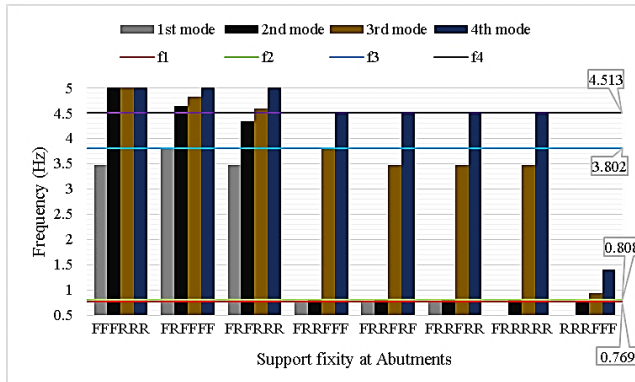


Figure 3: Frequency versus support fixity at abutments

When two of the translation movements are restrained at abutments, fundamental frequencies exceed the thresholds. However, when only one translational movement is fixed, the results are more close to initial values (see Figure 3). Furthermore, when full rotation is allowed or restricted in three directions, modal data changes considerably. Better agreement is observed when at least one of the rotational axis is released. Neoprene bearing used at abutments is a single layer elastomeric bearing with two bearing pedestals. Elastomers accommodate translational and rotational deformations, since they are very flexible in shear [13]. When elastomers are subjected to high compressive force, they expand laterally which result in deformation in the direction of expansion [11]. Neoprene bearings at abutments have no reinforcement and are made of plain elastomer pads, hence only bulging force due to friction is controlled. It can be assumed that the fixity of supports at abutments lie between FRRFFF and FRRFRR.

In the same vein, when rotational deformations are restrained for pier bearing, the results changed dramatically and very small frequencies are observed. Moreover, supports with free rotational deformation showed more consistent results. Rocker bearings are normally used to transmit horizontal forces and can provide rotational motion about two axes [13]. Hence, it can be postulated that three rocker bearings at pier transmit the forces from superstructure since the pier is cast integrally with deck. Due to monolithic fixity of pier and deck, rotational deformation is allowed to act at bearing joints to prevent slippage. Thus, the fixity of pier bearings lie in the region between FFFRRR and FFRRRR.

3 FIELD TEST SIMULATION

Primary dynamic analysis of the bridge can significantly aid in selecting suitable field testing procedure by considering the initial FEM modal data. In ambient vibration testing (AVT), in-situ dynamic behaviour of bridge in its normal service is captured without interrupting traffic which is a desirable choice for bridge condition assessment in contrast to conventional truck loading. Excitation was applied as ground motion (micro-tremor) to have broad-banded excitation for all frequencies of interest and to prevent any damage to structure.

Although very extensive sensor positioning techniques are available in the literature, e.g. [14, 15], such techniques are time-consuming and require iteration, particularly for large structures with a large number of degrees of freedom. Since only global modal behaviour of bridge is the main focus, acceleration record is considered as the output of sensors. Acceleration due to simulated traffic induced-vibration was exported to ARTeMIS to perform modal analysis [16]. Using trial and error, several sensor positioning systems were tested as shown in Figure 4. Consideration was paid to minimal instrumentation cost, installation difficulties and need for traffic closure for specifying optimum layout. Also, locating sensors at nodal points was

avoided, where minimum amplitude of vibration occurs. Taking all these into account and based on the excited mode shapes, a total of 12 sensors with average spacing of 6.3m was found to be suitable (Figure 4-G). At northern kerb (cantilever footway), six uniaxial accelerometers are placed. In the southern kerb, six biaxial accelerometers are positioned to capture the lateral and torsional modes. Since the bridge is considered as a rigid body, the motion of points between sensor points will be calculated by defining linear interpolation between sensor locations for mode shape display.

In the axiom of operational modal analysis, data are treated in time-domain or frequency domain. To cross-validate results for quality control, three frequency domain methods, viz. Frequency Domain Decomposition (FDD), Enhanced Frequency Domain Decomposition (EFDD) and Curve-fit Frequency Domain Decomposition (CFDD) were used for modal parameter estimation. In addition, three time domain Stochastic Subspace Identifications (SSI) data-driven algorithms, namely SSI Principle Component (SSI-PC), SSI Canonical Variate Analysis (SSI-CVA) and SSI Unweighted Principle Component (SSI-UPC) were used as well. For brevity, the aforementioned modal estimation methods are not explained and further reading can be found in [19].

Estimated mode shapes are illustrated in Figure 5. Except the fifth mode, other mode shapes are anti-symmetric. Oscillation of six mode shapes match well with the free vibration analysis, which means that the proposed sensor orientations is appropriate for detecting lower-order modes, even for decoupling lateral modes.

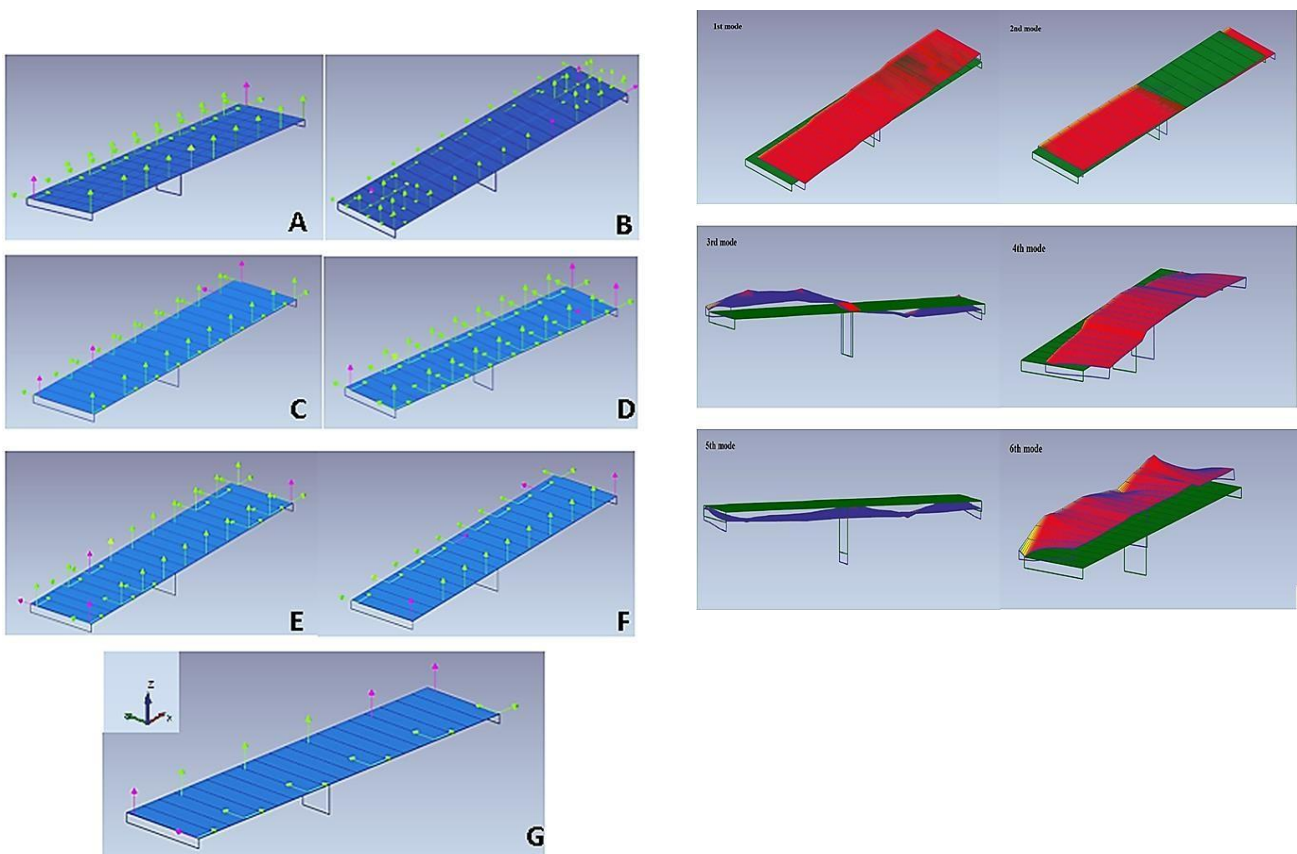


Figure 4: Sensors grid systems

Figure 5: Mode shapes obtained by modal analysis

Table 2: Identified modal parameters by different techniques

Mode number	1000 seconds (10% noise)						2000 seconds (20% noise)					
	Frequency Domain			Time Domain			Frequency Domain			Time Domain		
	FD D	EFD D	CFD D	SSI - PC	SSI- CVA	SSI - UP C	FDD	EFD D	CFD D	SSI - PC	SSI - CV A	SSI - UP C
1	0.78 1	0.78	0.78	0.77 6	0.76 7	0.766	0.781	0.78	0.78	-	0.77 1	0.77 2
2	-	-	-	0.81	0.81 5	0.819	-	-	-	0.80 3	0.81 4	0.81 5
3	-	-	-	3.77	3.82 7	3.821	-	-	-	3.85 2	3.82 6	3.83 5
4	4.54	4.52	4.52	4.49 7	4.50 2	4.473	4.54	4.52	4.52	4.50 6	4.51	4.50 4
5	5.32	5.32	5.32	5.31 3	5.32 9	5.329	5.27	5.27	5.27	5.33 3	5.33 7	5.33 6
6	8.8	8.9	8.9	8.85 6	8.82 9	8.867	8.8	8.9	8.9	8.85 9	8.86	8.86 2

A total of 100,000 and 200,000 time-series acceleration data were generated for 1000 sec and 2000 sec test setups respectively (see Table 2). To account possible errors in measurement and to investigate the effectiveness of sensors grid system and signal processing techniques, both test setup data were contaminated with random noise. It is apparent that time domain methods have advantage over the frequency domain methods in modal parameter identification.

All three frequency algorithms could not identify the second lateral mode and first bending mode. On the other hand, all three SSI-data driven techniques recognized all modes. First two lateral mode shapes are closely spaced and could be decoupled by SSI methods. SSI-PC in 2000 seconds missed the first mode, which is due to high damping ratio (20.1%) that exceeded the range of 0-7.5% damping. In traffic excitation, damping value is dependent on amplitude and level of excitation which bias the recorded

damping [17, 18]. Owing to this, 5% constant damping was assumed in initial FEM while damping values from modal analysis are not reported here. An example of stabilization diagram for subspace model (SSI-UPC) is shown in Figure 6.

Frequency domain methods perform well when mode shapes are well separated, since structural mode shape estimation is based on power spectral density peaks [20, 21]. If resolution of singular value decomposition (SVD) peaks is not detected, then the mode shape remains unidentified.

This can be further illustrated in Figure 7, whereby below 10 Hz only four peaks are barely

visible. Second lateral mode is closely spaced in the realm of first mode without clear SVD peak, so is not identified. Even though first bending mode has clear peak in green line which is SVD attributed to one of projection channels, it could not be detected by other SVD matrix and hence remained unidentified. Conversely, SSI-data driven methods detected modes even when the peaks are not distinct. This indicates the reliability of SSI in capturing closely spaced and lower order mode shapes [22-24].

taken as 2000 sec. Frequency regions with red colour indicate most energy and regions with dark blue have the least energy. It is explicitly notable that sufficient energy exists within 10 Hz which lasts for entire measurement time. This means that applied excitation was quite adequate, because frequencies of interest for bridge occur within 0 to 10 Hz.

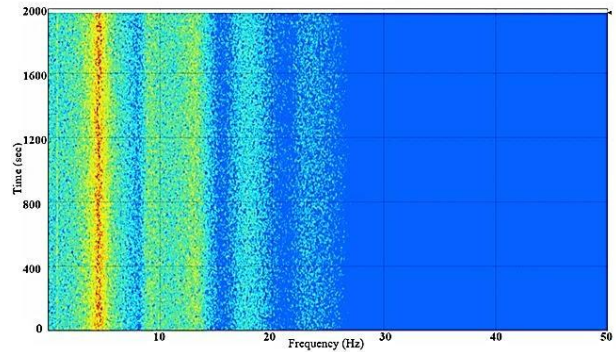


Figure 8: Spectrogram of first and last biaxial accelerometer in Y direction

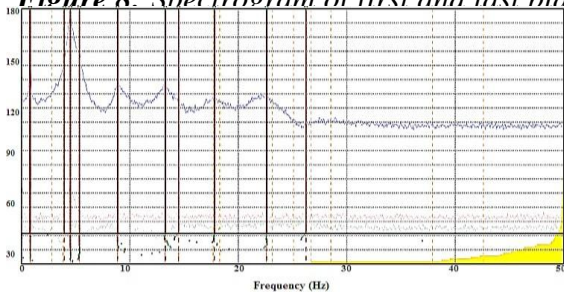
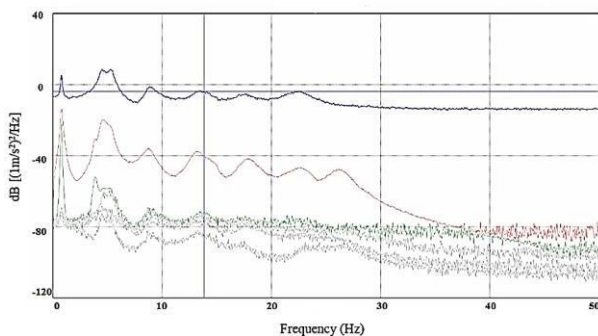


Figure 6: Stabilization diagram of state space model for 2000sec test setup (SSI-UPC)



formation and then points out to either imaginary or real values of oscillation due to vibration coincide, otherwise, the mode shape is said to be imaginary which is due to bad-quality measurements and time-varying data. A mode has value of one.

Table 3: Percentage of modal complexity factors

Test setup	MCF for mode shapes (%)					
	1	2	3	4	5	6
1000 sec						
SSI-PC	52.5	1.8	28.4	0.36	0.008	0.16
SSI-CVA	35.2	0.52	35.55	0.23	0.02	0.02
SSI-UPC	45.6	1.4	1.27	0.01	0.01	0.05
2000 sec						
SSI-PC	-	7.1	12.82	0.10	0.02	0.04
SSI-CVA	79.0	0.8	5.24	0.10	0.002	0.01
SSI-UPC	73.4	1.6	15.49	0.10	0.01	0.06

Figure 7: Singular value decomposition of spectral densities for 2000sec test setup

To explore the adequacy of the excitation source, magnitudes of data time-series between sensors located at abutments are displayed. Graph in Figure 8 is called spectrogram, which is visual representation of energy variations in frequency region. This spectrogram is between uniaxial sensors located at beginning of span one and end of span two. Horizontal axis represents the frequency range, which is taken from 0 to 50 Hz. The vertical axis shows the measurement time, which is

It can be seen from Table 3 that all modes identified have Modal Complexity Factor (MCF) percentage close to zero, except for first mode which shows very high percentage of MCF. This is due to the lateral movement of first mode which has close natural frequency with second mode [25]. It can be stated that identified mode shapes are true mode shapes of bridge which ascertain the assumption of lightly-damped structure in FE model.

4 CONCLUSIONS

Despite the fact that limited technical data was available, best engineering judgment was practiced to develop a detailed FEM of bridge to simulate its dynamic behaviour. FEM was developed based on design drawings and effects of different parameters on modal behaviour of bridge were investigated. Results indicated that for initial FEM, support conditions in abutment and pier can substantially alter the dynamic response. In case that boundary conditions are uncertain, parametric study as shown can be conducted to find out the suitable fixity conditions. Besides, any change in girders cross sections must be included in FEM to account for change in fundamental frequencies and mode shapes. Initial FEM served as baseline for estimation of bridge global dynamic response in the undamaged state.

Findings from initial FEM, while preliminary, identified the controlling parameters to be considered before and after model updating for box girder bridges made with reinforced concrete. Additional FEM of RC box girder bridge with different lengths will be studied to further the findings.

For actual field test, wireless accelerometers with sensitivity range of ± 1.0 V/g could be glued to the sides of bridge using quick-setting epoxy to prevent movement of sensors during measurement. Other sensor types such as strain gages and Fibre Bragg Grating can be positioned using initial FEM data if additional information is needed. Data acquisition system with anti-aliasing feature and sufficient data storage is suitable for receiving measurements from sensors. Sampling rate of 100 Hz with minimum acquisition time of 1000 sec is adequate to excite the frequency range of interest (below 10 Hz). Since the bridge is lightly damped, traffic excitation can easily excite the low order (early) frequencies. Based on the initial modal analysis, SSI-data driven techniques performed better in decoupling lower order modes and prevailed over frequency domain methods in mode shapes identification.

In the next stage of this study, using the suggested field test scheme, ambient vibration test will be performed. The analysis of theoretical model undertaken here, acts as a checking tool for reliability of recorded experimental data for model updating using identified parameters. Refined FEM will serve as baseline model for subsequent inspections and maintenance needs, and will enable the provision of retrofit solutions and load rating.

REFERENCES

- [1] Logistics Association of Australia: Supply Chain Report. Logistics Association of Australia Ltd., 2011.
- [2] American Association of State Highway and Transportation Officials: AASHTO LRFD

- bridgedesign specifications. Washington, D.C., 2012.
- [3] Australian Standards: Bridge Design part 5: Concrete (AS 5100.5). Sydney, 2004.
- [4] Queensland Department of Transport and Main Roads: Tier 1 Heavy Vehicle Bridge Assessment Criteria. TMR, 2013.
- [5] J. M. Brownjohn, E. Caetano, and A. A. Cunha: Civil structure condition assessment by FE model updating: methodology and case studies. *Finite Elements in Analysis and Design*, 37(10):761-775, 2011.
- [6] Y. Yang and L.P. Wang, Finite element model updating method and its application. In *23rd Conference and Exposition on Structural Dynamics, IMAC-XXIII*, 2005.
- [7] S. Živanović, A. Pavic, and P. Reynolds: Modal testing and FE model tuning of a lively footbridge structure. *Engineering Structures*, 28(6): 857-868, 2006.
- [8] D. Ewins. Model validation: Correlation for updating. *Sadhana*, 25(3): 221-234, 2000.
- [9] American Association of State Highway Officials: AASHTO Standard Specifications for Highway Bridges. Washington, D.C., 1970.
- [10] A. Krimotat and L. H. Sheng. Chapter 8: Structural Modelling. In Wai-Fah and L. Duan, editors, *Bridge Engineering Handbook*, CRC press, 2014.
- [11] M. Pezeshpour, L. Duan and P. Chung. Chapter 4: structural modelling and analysis, *Bridge Design Practice*, California Department of Transportation, 2015.
- [12] Parke, G. and N. Hewson: ICE manual of bridge engineering, Thomas Telford, London, 2008.
- [13] L. Hong-Nan Li, Y. Ting-Hua, L. Ren, D. S. Li, and Lin-Sheng Huo: Reviews on innovations and applications in structural health monitoring for infrastructures. *Structural Monitoring and Maintenance*, 1(1): 1-45, 2014.
- [14] H. Sohn, C. R. Farrar, F. Hemez, D. D. Shunk, D. W. Stinemas, B. R. Nadler and J. J. Czarnecki: A review of structural health monitoring literature: 1996-2001. Los Alamos National Laboratory: Los Alamos, 2004.
- [15] Structural Vibration Solutions A/S: ARTeMIS Modal Release 4.0.05. Aalborg East, Denmark, 2015.
- [16] M. F. Green. Modal test methods for bridges: A review. In *13th International Modal Analysis Conference (IMAC)*, 1995.